Available online at www.sciencedirect.com
SCIENCE DIRECT®
Journal of Photochemistry and Photobiology A: Chemistry 168 (2004) 103–108
Journal of Photochemistry and Photobiology A:Chemistry
www.elsevier.com/locate/jphotochem

Kinetic and mechanistic study of the F atom reaction with nitrous acid

Yuri Bedjanian*, Stéphane Lelièvre, Georges Le Bras

Laboratoire de Combustion et Systèmes Réactifs, CNRS and Université d'Orléans, 1c Avenue de la Recherche Scienti., 45071 Orléans Cedex 2, France

Received 27 April 2004; received in revised form 21 May 2004; accepted 24 May 2004
Available online 3 July 2004

Abstract

The kinetics and mechanism of the reaction of nitrous acid (HONO) with F atoms have been studied using the mass spectrometric discharge-flow method at 298 K and at a total pressure of 130 Pa of helium. The rate coefficient of the reaction F + HONO → products (1) was measured under pseudo-first order conditions from the kinetics of HONO decay in excess of F atoms: $k_1 = (5.4 \pm 1.1) \times 10^{-11}$ cm^3 molecule^{-1} s^{-1} (quoted uncertainty includes estimated systematic errors). NO_2 was detected as a product of reaction (1) and the reaction F + HONO → HF + NO_2 (1a) was found to be the main (if not unique) channel of reaction (1) under the experimental conditions of the study ($k_{1a}/k_1 = 1.0 \pm 0.1$ ($\pm 2\sigma$)). These results indicate that reaction (1) can be a suitable titration reaction for the measurements of the absolute HONO concentrations under laboratory conditions.

Keywords: Reaction; Kinetics; Rate constant; Nitrous acid; HONO; F

1. Introduction

Nitrous acid (HONO) is an important atmospheric species, particularly due to its potential influence on the oxidation capacity of the atmosphere, since the photolysis of HONO to NO and OH (major oxidant in the troposphere) enhances photooxidation processes, e.g. [1], including tropospheric ozone formation:

$$HONO + h\nu\,(300\text{–}390\,nm) \rightarrow OH + NO$$

Currently it is accepted that atmospheric HONO is produced mainly via heterogeneous reactions, although it is not clear whether HONO is produced mainly on the surface of aerosols [2,3] or on the ground [4]. In addition, the mechanisms leading to HONO formation are still not completely understood.

The flow tube kinetic and mechanistic investigations of the heterogeneous reactions leading to conversion of nitrogen compounds into HONO are currently under way in our group. The study is focused on HONO formation and loss processes on soot. To better determine the yield of HONO from heterogeneous reactions one need a well characterized source of HONO and a method for the determination of the absolute concentrations of this species in the flow reactor. We report here a kinetic and mechanistic study of the elementary reaction of fluorine atoms with HONO, which is a potential candidate for use as a titration reaction for the determination of the absolute concentrations of HONO in laboratory studies:

$$F + HONO \rightarrow \text{products} \quad (1)$$

2. Experimental

Experiments were carried out in a discharge flow reactor using a modulated molecular beam mass spectrometer as the detection method. The main reactor, shown in Fig. 1 along with the movable injector for the reactants, consisted of a Pyrex tube (45 cm length and 2.4 cm i.d.). The walls of both the reactor and the injector were coated with halocarbon wax to minimize the heterogeneous loss of active species. All experiments were conducted at $T = 298$ K and 130 Pa total pressure, helium being used as the carrier gas.

F atoms were generated in a microwave discharge of F_2 diluted in He. To reduce F atom reactions with glass surface inside the microwave cavity, a ceramic (Al_2O_3) tube was inserted in this part of the injector. It was verified by mass spectrometry that more than 90% of F_2 was dissociated in the microwave discharge. The fluorine atoms were detected

* Corresponding author. Tel.: +33 2 38255474; fax: +33 2 38696004.
E-mail address: bedjanian@cnrs-orleans.fr (Y. Bedjanian).

1010-6030/$ – see front matter © 2004 Elsevier B.V. All rights reserved.
doi:10.1016/j.jphotochem.2004.05.021

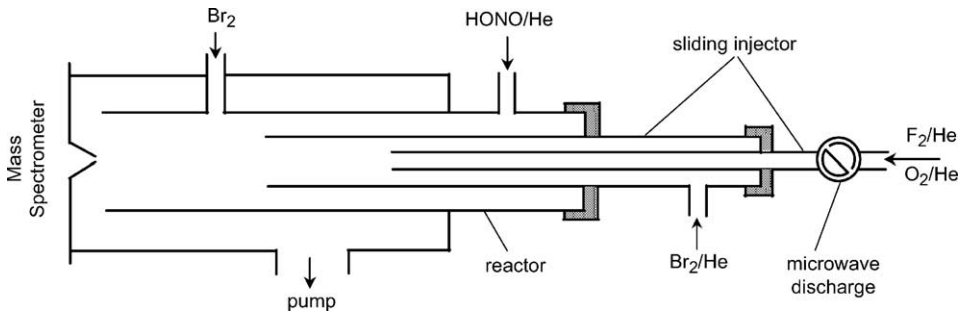

Fig. 1. Diagram of the flow reactor used.

at their parent peak (F^+, $m/e = 19$) and also as FBr^+ at $m/e = 100$, after scavenging by Br_2 at the end of the reactor through the fast reaction [5]:

$$F + Br_2 \rightarrow FBr + Br,$$
$$k_2 = 2.2 \times 10^{-10}\,cm^3\,molecule^{-1}\,s^{-1} \quad (2)$$

(all rate constants are given at $T = 298$ K). Br_2 was added 5 cm upstream of the sampling cone.

The advantage of this last method of F atom detection compared with the direct detection at $m/e = 19$ (F^+) is that one does not need to make corrections on the possible contribution of HF, product of reaction (1), at $m/e = 19$. All the other relevant species were detected at their parent peaks: $m/e = 38$ ($F_2{}^+$), 47 ($HONO^+$), 46 ($NO_2{}^+$), 30 (NO^+), 160 ($Br_2{}^+$), 36 (HCl^+).

Absolute concentration of F atoms was measured from the titration reaction (2) using an excess of Br_2. In this case, $[F] = \Delta[Br_2] = [FBr]$. The concentrations of the stable species in the reactor were calculated from their volumic flow rates obtained from the measurements of pressure drop of mixtures of the species with helium in calibrated volume flasks.

BrO radicals used to titrate NO potentially present in the HONO source (see below) were produced by reaction (3) [6]:

$$O + Br_2 \rightarrow BrO + Br,$$
$$k_3 = 1.4 \times 10^{-11}\,cm^3\,molecule^{-1}\,s^{-1} \quad (3)$$

The O atoms were generated from microwave discharge in O_2/He mixtures. BrO radicals were detected at their parent peaks at $m/e = 95/97$ as BrO^+. The determination of their absolute concentrations consisted in the usually used procedure of BrO titration with an excess NO with simultaneous detection of NO_2 formed ($\Delta[BrO] = \Delta[NO_2]$) [7]:

$$BrO + NO \rightarrow Br + NO_2,$$
$$k_4 = 2.1 \times 10^{-11}\,cm^3\,molecule^{-1}\,s^{-1} \quad (4)$$

HONO was generated via heterogeneous reaction of HCl with $NaNO_2$:

$$HCl + NaNO_2 \rightarrow HONO + NaCl \quad (5)$$

HCl diluted in He was flowed through a column containing $NaNO_2$ crystals and heterogeneously formed HONO was injected through the reactor sidearm (Fig. 1) and detected at its parent peak as $HONO^+$ ($m/e = 47$). Absolute concentrations of HONO were measured in situ using the method proposed in the present study. This direct calibration method uses the title reaction $F + HONO \rightarrow HF + NO_2$ (mechanistic information from this study is given below) and consists of the chemical conversion of HONO to NO_2 which can be easily calibrated ($\Delta[HONO] = \Delta[NO_2]$).

Under the experimental conditions used this source of HONO was found to be free of residual concentration of HCl. The monitoring of HCl concentration by mass spectrometry confirmed that HCl was completely consumed in reaction with $NaNO_2$ and did not reach the main reactor. It was observed that concentration of HONO formed was in the range of 10–20% of HCl consumed. Fig. 2 shows an example of the dependence of the concentration of HONO formed in reaction (5) on the concentration of HCl consumed. For this example the yield of HONO is near 14%.

The HONO source was found to be free of NO_2 and

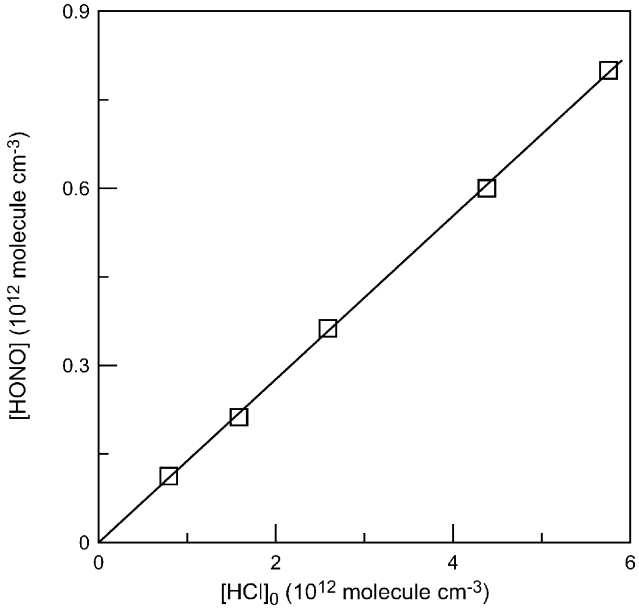

Fig. 2. Dependence of the concentration of HONO formed on the concentration of HCl consumed in the column containing $NaNO_2$ crystals.

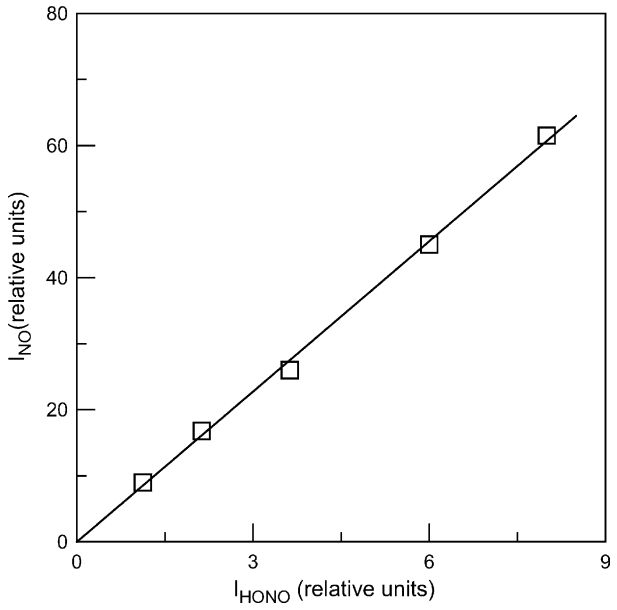

Fig. 3. Dependence of the mass spectrometric signal intensity observed at $m/e = 30$ on the signal intensity at $m/e = 47$ ($HONO^+$).

HNO_3: no signals were detected at $m/e = 46$ (NO_2^+), 63 (NO_3^+) and 64 (HNO_3^+). The impurity concentration of NO_2 from the source of HONO was estimated to be less than $0.04 \times$ [HONO]. On the other hand, a very intense signal at $m/e = 30$ (NO^+) (by a factor of 7.5 higher than that of HONO at $m/e = 47$) coming from the source of HONO was detected (Fig. 3). Two possibilities can be considered for the origin of the mass spectrometric signal at $m/e = 30$: contribution due to the fragmentation of HONO in the ion source of the mass spectrometer or NO formation in the source of HONO (for example, by heterogeneous decomposition of HONO). To distinguish between theses two possibilities specific experiments have been carried out. The idea of these experiments was to introduce BrO radicals into the reactor to convert the NO molecules (if present in the reactor) to NO_2 via reaction (4) and to measure in this way the number of NO molecules coming as impurity from the HONO source. BrO radicals formed in reaction of O atoms with excess Br_2 (reaction (3)) were introduced into the reactor through the movable injector, HONO being flowed through the reactor sidearm. It has to be noted first that no HONO consumption was observed for the maximum reaction time of $\approx 1.5 \times 10^{-2}$ s and mean concentration of BrO around 10^{13} molecule cm^{-3}. This mean concentration takes into account a 40–50% decrease of BrO concentration observed due to the BrO + BrO reaction [7]:

$$\text{BrO} + \text{BrO} \rightarrow \text{products}, \quad k_6 = 3.2 \times 10^{-12}\,\text{cm}^3\,\text{molecule}^{-1}\,\text{s}^{-1} \qquad (6)$$

This allowed to set an upper limit for the rate constant of the reaction between BrO radicals and HONO:

$$\text{BrO} + \text{HONO} \rightarrow \text{products}, \quad k_7 < 3 \times 10^{-13}\,\text{cm}^3\,\text{molecule}^{-1}\text{s}^{-1} \qquad (7)$$

The same conclusion holds for the reactions of HONO with Br atoms (formed in reactions (3) and (6) and present in the reactor at concentrations higher that those of BrO) and with Br_2 (precursor of BrO, present in the reactor at concentrations around 3×10^{13} molecule cm^{-3}). In contrast to HONO, the concentrations of NO and NO_2 were found to be affected by the addition of BrO into the reactor. As expected we observed a decrease of the signal intensity at $m/e = 30$ and increase of that at $m/e = 46$, attributed to the NO consumption and NO_2 formation in reaction (4), respectively. Moreover, the NO concentration consumed and NO_2 concentration formed were found to be equal within 5%. These experiments allowed to determine that the HONO sample contained approximately 15% NO impurity: [NO] = $(0.15 \pm 0.04) \times$ [HONO].

The purities of the gases used in the study were as follows: He > 99.9995% (Alphagaz) was passed through liquid nitrogen traps; Br_2 > 99.99% (Aldrich); F_2 (5% in helium, Alphagaz); HCl—5% mixture in He (Praxair); O_2 > 99.995% (Alphagaz); NO_2 > 99% (Alphagaz); NO > 99% (Alphagaz), purified by trap-to trap distillation to remove NO_2 traces.

3. Results and discussion

Two series of experiments were performed: in the first one rate constant of reaction (1) was measured by monitoring the HONO consumption kinetics in excess of F atoms and in the second one the reaction products were studied.

3.1. Rate constant measurement

Reaction (1) was studied under pseudo-first-order conditions using an excess of F atoms over HONO. The initial concentrations of HONO were in the range $(1.9–4.0) \times 10^{11}$ molecule cm^{-3}; the concentration of excess F atoms was varied between 0.08 and 1.40×10^{13} molecule cm^{-3}. Flow velocity in the reactor was 1720–1780 cm s^{-1}. The consumption of excess reactant, F atoms, was negligible (<15%) in most of the experiments, however it reached up to 50% in a few kinetic runs. This consumption of F atoms was due to reaction with HONO, heterogeneous loss and reaction with traces of water present in the reactor. In the calculation of the rate constant k_1 the F atom concentration have been kept constant, with a mean value along the HONO decay kinetics. A numerical simulation of the HONO decay kinetics, using the observed [F] temporal profiles, gave the same values for k_1 (within 5%).

An example of kinetic runs of the exponential decay of HONO measured with different concentrations of F atoms is shown in Fig. 4. The values of the pseudo-first-order rate

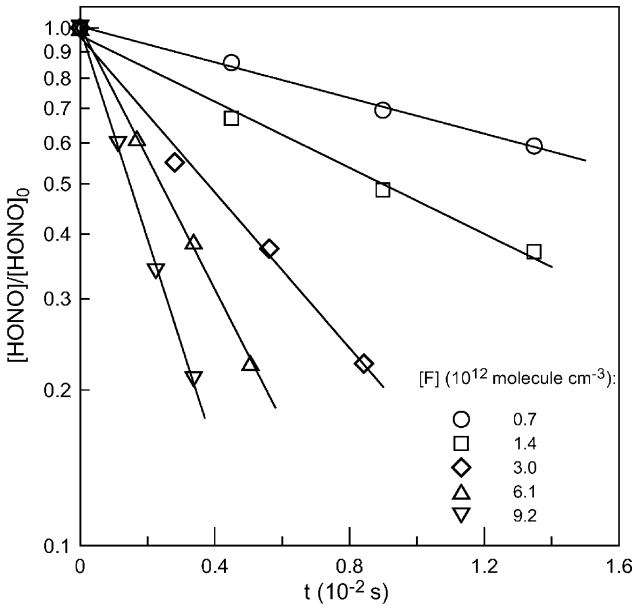

Fig. 4. Examples of the kinetic runs of HONO consumption in reaction with excess F atoms.

constants, $k_1' = -\mathrm{d}(\ln[\mathrm{HONO}])/\mathrm{d}t$, determined from the kinetics of HONO consumption were corrected for axial and radial diffusion of HONO [8]. The diffusion coefficient of HONO in He was calculated from that of CO_2 in He [9]. Typical corrections were within 10%.

Fig. 5 shows the dependence of the pseudo-first-order rate constant, $k_1' = k_1 \times [\mathrm{F}]$, on the concentration of F atoms. The negligible zero-intercept is in good agreement with the experimental observation that no change in HONO concentrations was observed in the absence of F atoms (discharge of F_2/He off) when the injector was moved. The value of k_1 obtained from the slope of the linear least square fit to the experimental data is: $k_1 = (5.4 \pm 0.1) \times 10^{-11}\,\mathrm{cm^3\,molecule^{-1}\,s^{-1}}$ with 1σ statistical uncertainty. Finally recommended value of k_1 from this study is:

$$k_1 = (5.4 \pm 1.1) \times 10^{-11}\,\mathrm{cm^3\,molecule^{-1}\,s^{-1}}$$

The uncertainty of k_1 represents the combination of statistical and estimated systematic errors. The estimated systematic uncertainties include ±5% for flow meter calibrations, ±3% for pressure measurements and ±15% for measurements of the absolute concentrations of fluorine atoms. Combining these uncertainties in quadrature and adding 2σ statistical uncertainty yields the quoted near 20% uncertainty on k_1.

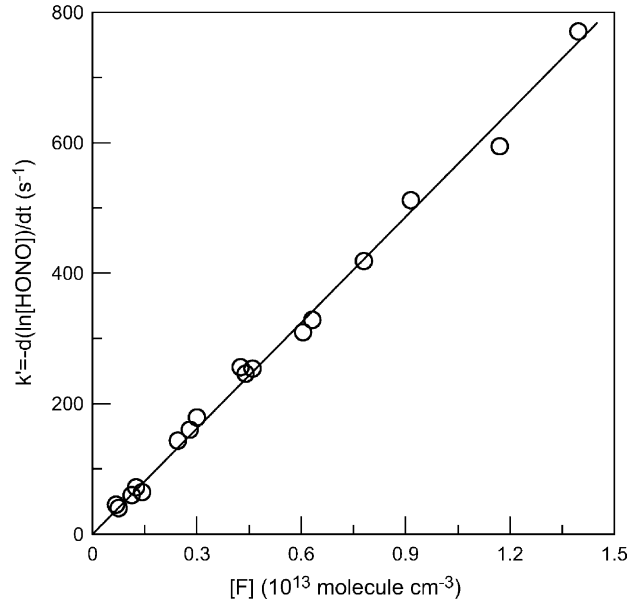

Fig. 5. The pseudo-first order plot of HONO consumption in reaction with excess F atoms.

3.2. Products study

The possible channels of reaction (1) are the following:

$$\mathrm{F + HONO \rightarrow HF + NO_2},\quad \Delta H_\mathrm{r} = -57.2 \pm 0.3\,\mathrm{kcal\,mol^{-1}} \tag{1a}$$

$$\mathrm{F + HONO \rightarrow OH + FNO},\quad \Delta H_\mathrm{r} = -6.7 \pm 2.1\,\mathrm{kcal\,mol^{-1}} \tag{1b}$$

$$\mathrm{F + HONO \rightarrow NO + FOH},\quad \Delta H_\mathrm{r} = -1.8 \pm 1.1\,\mathrm{kcal\,mol^{-1}} \tag{1c}$$

$$\mathrm{F + HONO \rightarrow FO + HNO},\quad \Delta H_\mathrm{r} = 51.6 \pm 4.1\,\mathrm{kcal\,mol^{-1}} \tag{1d}$$

Enthalpy data are from [7]. Channel (1d) can be excluded under the experimental conditions of the present study as too endothermic to proceed with the high k_1 rate constant measured. Analysis of the mass spectra of the products of reaction (1) led to the observations of the peaks at $m/e = 30$ (NO^+) and 46 ($m/e = NO_2^+$) in the presence of reaction.

Concerning channel (1b), no evidence was found for the formation of neither FNO or OH radicals in reaction (1). First, no signal at $m/e = 49$ (FNO^+) was observed, however, FNO possibly formed in reaction (1) could give a most intense peak at $m/e = 30$ (NO^+) due to fragmentation in the ion source of the mass spectrometer. To try to detect OH, co-product of FNO in reaction (1b), Br_2 in concentrations $(3–5) \times 10^{13}\,\mathrm{molecule\,cm^{-3}}$ was added at the downstream end of the reactor (see Fig. 1). In this case, the OH radicals, if formed in reaction (1b), could be converted to HOBr and detected at $m/e = 96$ ($HOBr^+$) [10]:

$$\mathrm{OH + Br_2 \rightarrow Br + HOBr},\quad k_8 = 4.0 \times 10^{-11}\,\mathrm{cm^3 molecule^{-1}\,s^{-1}} \tag{8}$$

On the other hand it should be noted that the experiments were carried out in excess of F atoms over HONO. Under theses conditions, OH radicals, if formed, could react with excess F atoms via reaction (9):

$$F + OH \rightarrow O + HF \quad (9)$$

However, even in this case the presence of Br_2 would convert O atoms into BrO (reaction (3)), which could be easily detected at $m/e = 95/97$ (BrO^+). Finally, no product formation was observed at $m/e = 95/96/97$, allowing to exclude the significant contribution of reaction pathway (1b) under the experimental conditions of the study.

To distinguish between channels (1a) and (1c) one needed an independent absolute calibration of HONO to determine, for example, the branching ratio for the NO_2 forming channel (1a). To derive the absolute concentrations of HONO, specific experiments were carried out, where HONO was titrated (complete consumption) with F atoms in presence of atomic oxygen in the reactor ([O] $\approx 3 \times 10^{13}$ molecule cm^{-3}). In this case NO_2 formed in channel (1a) is converted to NO in reaction with O atoms [7]:

$$O + NO_2 \rightarrow NO + O_2,$$
$$k_{10} = 1.0 \times 10^{-11}\ \text{cm}^3\ \text{molecule}^{-1}\ \text{s}^{-1} \quad (10)$$

Thus all HONO molecules consumed in reaction (1) are converted to NO, directly via channel (1c) or via channel (1a) followed by reaction (10). The dependence of [NO] formed on concentration of HONO consumed in reaction (1) is shown in Fig. 6. This plot allows for the determination of the absolute concentrations of HONO from known concentration of NO. It is important to note that under conditions of these experiments the excess oxygen atoms do not react with HONO and have no influence on the distribution of the products of reaction (1):

$$O + HONO \rightarrow \text{products},$$
$$k_{11} < 1.0 \times 10^{-15}\ \text{cm}^3\ \text{molecule}^{-1}\ \text{s}^{-1} \quad (11)$$

Similarly, the termolecular reactions of F atoms with NO and NO_2 are too slow at the low pressure of the study to have a significant impact on the obtained results [7]:

$$F + NO + M \rightarrow FNO + M,$$
$$k_{12} = 1.8 \times 10^{-31}\ \text{cm}^6\ \text{molecule}^{-2}\ \text{s}^{-1} \quad (12)$$

$$F + NO_2 + M \rightarrow FNO_2 + M,$$
$$k_{13} < 6.3 \times 10^{-32}\ \text{cm}^6\ \text{molecule}^{-2}\ \text{s}^{-1} \quad (13)$$

The knowledge of the absolute concentrations of HONO allowed for the determination of the NO_2 yield from the reaction of F atom with HONO. The NO_2 concentration formed as a function of [HONO] consumed in reaction (1) is shown in Fig. 7. The slope of the straight line gives $[NO_2]_{formed}/[HONO]_{consumed} = 1.03 \pm 0.06(\pm 1\sigma)$, showing that the branching ratio for channel (1a) is near unity. Thus the major channel of F atom reaction with nitrous acid is the most exothermic one.

The present study of reaction (1) is the first to be reported, therefore the obtained results cannot be compared with those from literature. Analysis of the existing kinetic data for other reactions of HONO [12] shows that, as a rule, these reactions are slow at near ambient temperatures.

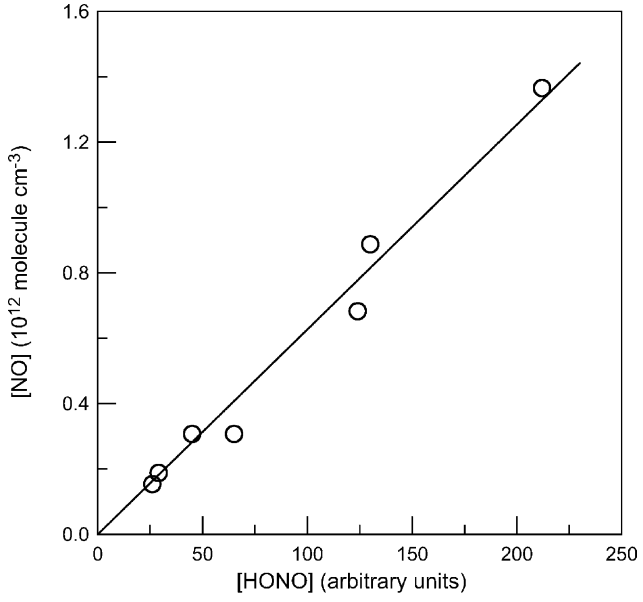

Fig. 6. Dependence of the concentration of NO formed on the concentration of HONO consumed in reaction (1) in the presence of oxygen atoms.

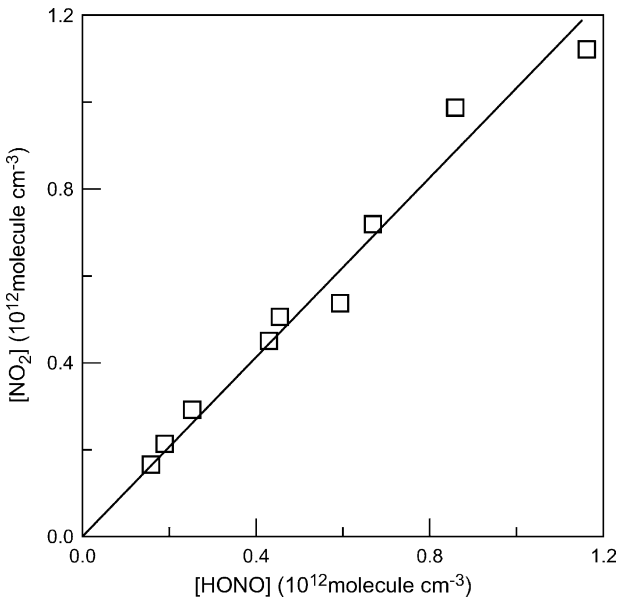

Fig. 7. Concentration of NO_2 formed in reaction (1) as a function of concentration of HONO consumed.

Thus, only upper limits were determined at $T = 298\,K$ for the rate constants of HONO reactions with atmospheric species such as HNO_3, NO_3, N_2O_5, O_3 and O atoms: 7×10^{-19} [13], 2×10^{-15} [13], 7×10^{-19} [13], 4.5×10^{-19} [14] and $1 \times 10^{-15}\,cm^3\,molecule^{-1}\,s^{-1}$ [11], respectively. The only known rapid reaction of HONO is the reaction with OH radicals. This reaction being a potentially important atmospheric process was intensively studied [12]. Currently recommended value of the rate constant is: $4.5 \times 10^{-12}\,cm^3\,molecule^{-1}\,s^{-1}$ [7]. The reaction of OH radicals with HONO proceed via abstraction of H atom from HONO and NO_2 formation, similarly to the reaction of F atom with HONO as found in the present study.

In conclusion, the information obtained for reaction (1) in the present work shows that this reaction is fast and leads to the formation of NO_2 with the branching ratio around unity. Consequently, this reaction can be used as a titration reaction for in situ determination of the absolute concentrations of HONO through the detection of the stable NO_2 product.

Acknowledgements

This study has been carried out within the NITROCAT project funded by the European Commission within the "Environment and Climate" Programme.

References

[1] R.M. Harrison, J.D. Peak, G.M. Collins, J. Geophys. Res. 101 (1996) 14429.
[2] G. Lammel, D. Perner, P. Warneck, in: G. Restelli, G. Angeletti (Eds.), Physico-Chemical Behaviour of Atmospheric Pollutants, Kluwer Academic Publishers, 1988, pp. 469–476.
[3] J. Notholt, J. Hjorth, F. Raes, Atmos. Environ. 26A (1992) 211.
[4] R.M. Harrison, A.N. Kitto, Atmos. Environ. 28 (1994) 1089.
[5] P.P. Bemand, M.A.A. Clyne, J. Chem. Soc., Far. Trans. II 72 (1976) 191.
[6] J.M. Nicovich, P.H. Wine, Int. J. Chem. Kinet. 22 (1990) 379.
[7] S.P. Sander, R.R. Friedl, D.M. Golden, M.J. Kurylo, R.E. Huie, V.L. Orkin, G.K. Moortgat, A.R. Ravishankara, C.E. Kolb, M.J. Molina, B.J. Finlayson-Pitts, Chemical Kinetics and Photochemical Data for Use in Stratospheric Modeling, Evaluation No.14, JPL Publication 02-25, NASA, Jet Propulsion Laboratory, Pasadena, CA, 2003.
[8] F. Kaufman, J. Phys. Chem. 88 (1984) 4909.
[9] T.R. Marrero, E.A. Mason, J. Phys. Chem. Ref. Data 1 (1972) 3.
[10] Y. Bedjanian, G. Le Bras, G. Poulet, Int. J. Chem. Kinet. 31 (1999) 698.
[11] E.W. Kaiser, S.M. Japar, J. Phys. Chem. 82 (1978) 2753.
[12] A compilation of kinetics data on gas-phase reactions, in: NIST Chemical Kinetics Database, Release 1.1, Standard Reference Database 17, Version 7.0 (Web Version).
[13] T.J. Wallington, S.M. Japar, J. Atmos. Chem. 9 (1989) 399.
[14] G.E. Streit, J.S. Wells, F.C. Fehsenfeld, C.J. Howard, J. Chem. Phys. 70 (1979) 3439.